



*J. Serb. Chem. Soc.* 87 (1) 133–144 (2022)  
JSCS–5510

## Characterization of landfill deposited sediment from dredging process during different maturation stages

MILOŠ DUBOVINA, NENAD GRBA\*<sup>#</sup>, DEJAN KRČMAR, JASMINA AGBABA<sup>#</sup>,  
SRĐAN RONČEVIĆ<sup>#</sup>, ĐURĐA KERKEZ<sup>#</sup> and BOŽO DALMACIJA<sup>#</sup>

*University of Novi Sad, Faculty of Sciences, Department of Chemistry, Biochemistry and Environmental Protection, Trg Dositeja Obradovica 3, 21000 Novi Sad, Serbia*

(Received 30 August, revised and accepted 29 November 2021)

**Abstract:** A long-term monitoring of deposited sediment in the environment is considered in order to examine the mechanism of incorporation of Cu and Cd into mineral fractions and to investigate their bioavailability during landfill maturation. Using the sequential extraction technique (Community Bureau of Reference, BCR), the dominant presence of Cu and Cd in the oxidation and residual fraction was determined, which suggests a low risk of bioavailability of these metals in the environment. The maturation of the deposited sediment indicates that the Cu and Cd content decreases over time in the exchangeable fraction and increases in the oxidation fraction. X-ray techniques XRF and EDS indicated a prevalence of silicates in the tested samples, which suggests the possibility of presence of silicate compounds that can bind metals and thus convert them into less mobile forms in the sediment. By imaging the samples with a scanning electron microscope SEM, the formation of heterogeneous structures over time was determined, which confirms the formation of new minerals and the potential possibility of incorporating copper and cadmium in them. In order to determine the mineral forms and dominant compounds in the examined sediment samples, X-ray diffraction analysis was applied, and the transformation pathways were explained.

**Keywords:** bioavailability of Cu and Cd in sediment fractions; metals adsorption, sequential extraction; sediment maturation mechanism.

### INTRODUCTION

In this research a structural characterization, heavy metals binding pathways with risk assessment of dredged riverbed sediment and determination of different maturation stages are presented. The deposited sediment samples from tree vertically hotspots landfill sites were subjected to long-term monitoring, over a period

\* Corresponding author. E-mail: nenad.grba@dh.uns.ac.rs

<sup>#</sup> Serbian Chemical Society member.

<https://doi.org/10.2298/JSC210830102D>

of 3 years (2017–2019) and become characterized as samples with variable values of heavy metals with the average composition (*e.g.*, Cu 245.15 mg/kg, Cd 9.16 mg/kg) mostly higher than of the upper continental crust (UCC).<sup>1,2</sup> In order to examine the bioavailability of high concentrations of Cu and Cd in the deposited sediment samples after dredging, an operational specification performed by the four-step BCR (Community Bureau of Reference) sequential extraction procedure was applied.<sup>3,4</sup> The structural characterization of the examined matrices using the scanning electron microscopy/energy dispersive X-Ray spectroscopy (SEM/EDS) and X-ray fluorescence analysis (XRF) characterized the qualitative and semi-quantitative distribution of elements that can represent an important instrumental analysis in order to determine the dominant binding mechanisms and mobility pathways of monitored metals in sediment system to stable forms.<sup>5,6</sup> X-ray diffraction (XRD) analysis determined the mineral forms of Cu and Cd, and in line with the analysis of other mineral forms present in the sediment, the mechanisms of potential metal adsorption were investigated.<sup>5</sup>

The general characterization of sediment using the mentioned techniques will contribute to the assessment of the risk of mobility of metal forms due to the influence of atmospheric precipitation, weathering reactions and leaching of sediment deposited on the landfill over long period of time.<sup>7</sup>

#### EXPERIMENTAL

The research area is positioned in the coastal area of the Bega Canal near the border with Romania. After the sludge was deposited in the environment, an exploratory landfill was formed, where long-term monitoring was performed for a period of 3 years (2017–2019). Risk assessment of metal mobility or distribution of heavy metals by fractions in sediment deposits after dredging was determined using the conventional technique of sequential sediment extraction (BCR).<sup>8-10</sup> The procedure for determining the distribution of heavy metals in sediments by fractions consists of four steps. In the first step, 1 g of a dry sediment sample is weighed and mixed with 40 mL of acetic acid (0.11 mol/L) in a 100 mL vessel and extracted for 16 h at 22±5 °C. The samples are then centrifuged; the supernatant is decanted and used for analysis. In the second step, the sediment from phase 1 is used in the second phase by adding 40 mL of hydroxylamine hydrochloride (0.5 mol/L) to the sample and extracting for 16 h at 22±5 °C. Centrifugation is then performed, the supernatant is decanted and the metal content is analysed. Samples from this phase are used in phase 3. In the third step, 10 mL of hydrogen peroxide (8.8 mol/L) is added; digestion is performed at room temperature for 1 h with occasional shaking. Evaporation for 1 h in a water bath at 85±2 °C to 3 mL. 10 mL of hydrogen peroxide (8.8 mol/L) is added, followed by digestion for 1 hour in a water bath at 85±2 °C, and then evaporated to a volume of 1 mL. 50 mL of 1 mol/L ammonium acetate is added and extraction continued for 16 h at 22±5 °C. The sample is centrifuged, the supernatant is decanted and used for analysis. Finally, in the fourth step, the samples from the third phase are subjected to digestion with imperial water (9 mL of HCl and 3 mL of HNO<sub>3</sub>), after which the samples are filtered and analyzed for metal content.

Qualitative and quantitative distribution of elements in sediment samples was analyzed using two different X-ray techniques by energy dispersive X-ray spectrometry (EDS) in combin-

ation with scanning electron microscopy (SEM) and X-ray fluorescence analysis (XRF). For SEM/EDS analysis, the samples were dried, and the entire volumes were ground into a fine powder. The powder sample was applied to the carbon strip and recorded. SEM analysis of samples was performed on Quantax 70 EDS System – Hitachi Tabletop Microscope TM3000 – Bruker, Germany. The X-ray fluorescence XRF process begins by homogenizing the sediment sample and recording it by measuring the wavelength or energy of the photon and the intensity of the characteristic radiation emitted from the sample. A Delta Premium Handheld XRF Analyzer Specifications analyzer was used to record sediment samples.

X-ray diffraction (XRD) is a widespread analytical technique that has been applied to determine different forms of crystal structures in sediment.<sup>11</sup> For X-ray diffraction analysis, the entire volume of sediment was crushed, and a certain amount of sample was applied to a glass plate, measuring 20 mm×20 mm and with a recess of 0.5 mm. Analyzes were performed on an automatic powder diffractometer Rigaku MiniFlex 600, Bragg–Brentano geometry with a secondary graphite monochromator. Recording was done in step mode, with a stop time of 2 s. Radiation was performed via copper anodes, with a voltage of 40 kV and a current of 15 mA.

#### RESULTS AND DISCUSSION

By using conventional sequential extraction (BCR), an assessment of the potential risk of deposited sediment into the environment after dredging activity was determined.<sup>12</sup> Long-term monitoring, over a period of 3 years (2017–2019), of sediment quality was determined analysing the binding of elevated metals, dominantly of copper and cadmium, to certain fractions of sediment in order to establish their bioavailability.

##### *Sediment related results from conventional sequential extraction (BCR) procedure*

The distribution of Cu and Cd (Figs. 1 and 2) show a dominant presence in the oxidable and residual phases, which suggests that these metals are mainly bound to organic matter, sulphides and minerals and therefore less available in the environment.<sup>13,14</sup> Individually inspection at each of the metal binding phases in the sediment, showed that copper is the most abundant in the residual fraction ranging from 44.42 to 50.95 %, while the binding to organic matter and sulphides

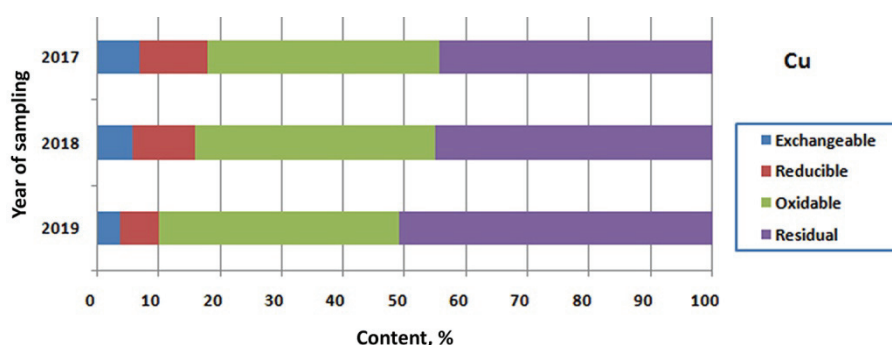


Fig. 1. Binding of Cu to different fractions during sediment maturation (2017–2019).

are also characterized by a high share of 37.51 to 38.92 % (Fig. 1). A similar trend of sediment binding is shown by Cd with a somewhat more dominant presence in the mineral fraction from 48.52 to 54.16 %, which indicates a low risk of bioavailability to biota (Fig. 2).<sup>15</sup>

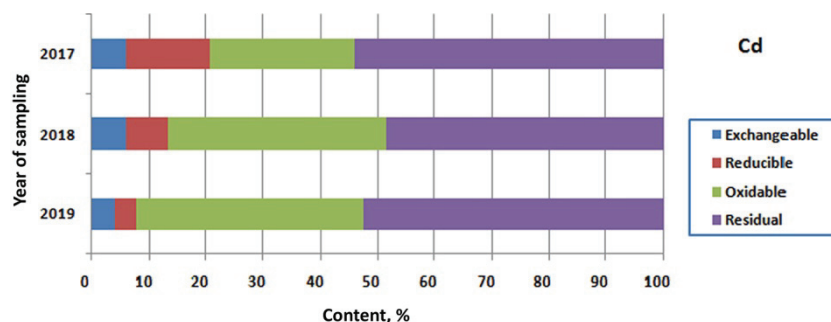


Fig. 2. Binding of Cd to different fractions during sediment maturation (2017–2019).

During long-term monitoring of sludge sediments, the percentage of Cu and Cd decreased in the dissolved phase (2018 (Cu 5.82 %; Cd 5.75 %), 2019 (Cu 3.90 %; Cd 3.70 %)), while the oxidative phase was characterized by a higher presence of these two metals. The change in the distribution of Cu and Cd in the sediment fractions indicates the formation of organic complexes and sulphides during the aging of the sediment at the landfill.<sup>16</sup>

#### *Semi quantitative to quality comparisons of different heavy metals indicators*

Comparison of XRF and EDS techniques and related results from XRF analysis of the hot spots of the investigated sediments (chronologically: S1 sample (2017), S2 sample (2018) and S3 sample (2019)), were scale up based on the increasing content of Si in the landfill sediment over time (Table I). The predominantly low Ca/Si ratio during all monitoring periods indicates sediment

TABLE I. Comparative quantitative spot analysis in selected areas of exploratory deposited samples using Energy dispersive X-ray spectrometry (EDS) and X-ray fluorescence analysis (XRF) techniques

Parameter	Year of characterization of deposited sediment					
	EDS			XRF		
	2017	2018	2019	2017	2018	2019
	Content, %					
Ca	1.89	1.21	0.89	1.72	0.93	1.89
Al	8.25	10.51	13.53	9.41	9.71	13.11
Si	18.59	22.72	24.35	20.92	23.64	25.21
	Atomic ratio					
Ca/Si	0.10	0.05	0.04	0.08	0.04	0.07
Si/Al	2.25	2.16	1.80	2.22	2.43	1.92

characterized by a high Si presence. Accordingly, the presence of Si suggests that silicate compounds predominate in the sediment, which is very important from the aspect of binding metals by silicate substances in the process of landfill maturation and thus reduces their mobility.<sup>5</sup>

The scanning electron microscopy shows a different microstructural nature or variations in the semi-homogeneous structure as well as visible macro/meso porosity. The formation of new minerals due to mineralogical changes is visible in Figs. 3–5 due to the formation of larger aggregates.

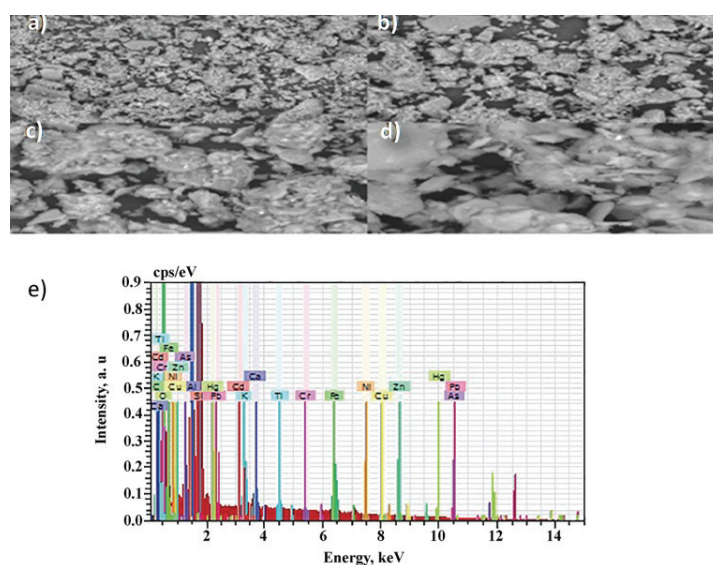


Fig. 3. Analysis of deposited sediment sample from 2017 using a scanning electron microscope (SEM) with magnification: a) 500×, b) 1000×, c) 2000×, d) 4000×; e) analysis of energy dispersive X-ray spectrometry (EDS).

The application of EDS and XRF analysis indicates that the sediment from 2019 has a slightly more heterogeneous structure, with a lower Si/Al ratio of about 1.80 (EDS) and 1.92 (XRF), respectively, compared to other periods of sediment characterization (Table I), which may also indicate a higher binding capacity of heavy metals during sediment landfill maturation.<sup>17</sup> This can also be explained by the presence of aluminosilicates with increased aluminium content.<sup>18,19</sup>

#### *Maturation and characterisation of sediments and heavy metals binding pathways*

As it was investigated in the geological classification of northern part of Serbia (Vojvodina) including cross-border geological units to Romania, the loess–paleosol section (LPS) of this region is dominantly represented and characterized by irregularities in sedimentological properties, magnetic susceptibility

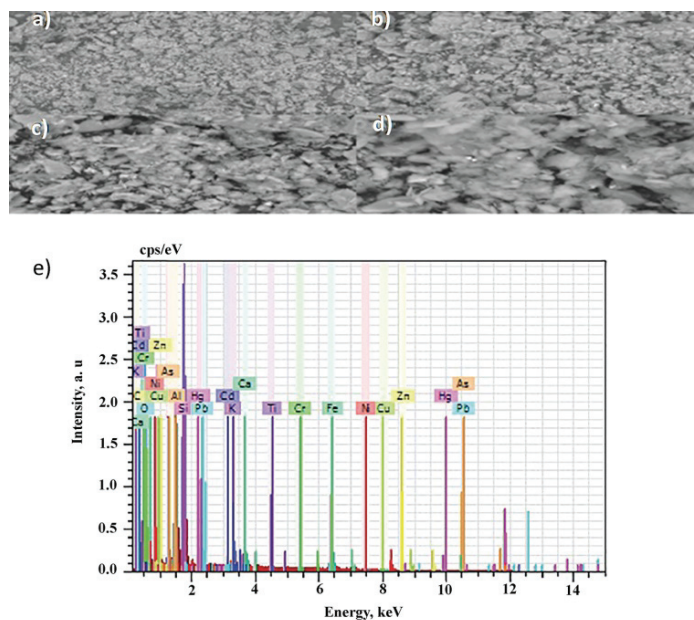


Fig. 4. Analysis of deposited sediment sample from 2018 using a scanning electron microscope (SEM) with magnification: a) 500 $\times$ , b) 1000 $\times$ , c) 2000 $\times$ , d) 4000 $\times$ ; e) analysis of energy dispersive X-ray spectrometry (EDS).

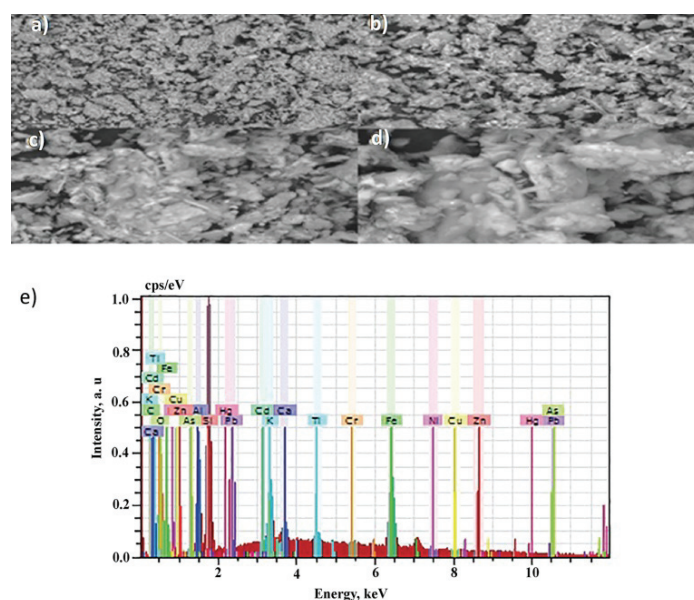


Fig 5. Analysis of deposited sediment sample from 2019 using a scanning electron microscope (SEM) with magnification: a) 500 $\times$ , b) 1000 $\times$ , c) 2000 $\times$ , d) 4000 $\times$ ; e) analysis of energy dispersive X-ray spectrometry (EDS).

and color of the sediment with a unique sedimentology differing from all other investigated sections in Serbia.<sup>20</sup> Characterization of three different time periods (2017–2019) by target samples using XRD analysis show elevated picks of minerals, shifting of high intensity of, *e.g.*, quartz to lower and alternating muscovite and albite (Fig. 6).

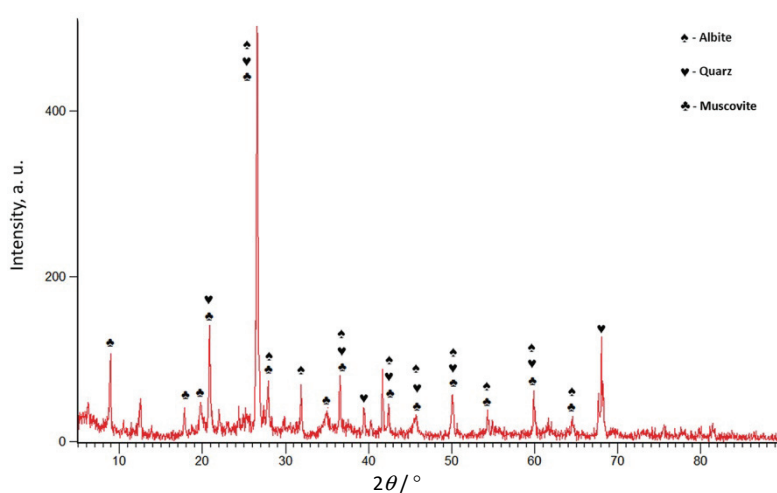


Fig. 6. The dominant selected minerals from sample 1 (2017).

Quartz ( $\text{SiO}_2$ ) and albite a sodium aluminosilicate ( $\text{NaAlSi}_3\text{O}_8$ ), Table II, are non-clay minerals and the albite as a feldspathic mineral can act as a sintering aid and sinter raw material at dominantly higher temperatures (rock forming mineral is possible also at 20 °C), 50 and 80 °C,<sup>21</sup> or pressure which can render the reactivity of it when exposed to an alkaline environment during the synthesis of the zeolite.<sup>22</sup>

TABLE II. Identified minerals in sample 1 (2017)

Compound name	Chemical formula
<b>Silicon oxide</b>	<b><math>\text{SiO}_2</math></b>
Copper indium sulfide	$\text{CuInS}_2$
Copper rhodium oxide	$\text{CuRh}_2\text{O}_4$
Copper oxide	$\text{Cu}_2\text{O}$
Copper telluride	$\text{Cu}_{2.8}\text{Te}_2$
Aluminum silicate	$\text{Al}_2\text{SiO}_5$
Potassium aluminum silicate hydroxide	$\text{KAl}_3\text{Si}_3\text{O}_{10}(\text{OH})_2$
<b>Sodium aluminum silicate</b>	<b><math>\text{Na}(\text{AlSi}_3\text{O}_8)</math></b>
Copper hydroxide sulfate hydrate	$\text{Cu}_{15}(\text{OH})_{22}(\text{SO}_4)_4(\text{H}_2\text{O})_6$

Albite may be most widely found in pegmatites and felsic igneous rocks such as granites. It was also found in low-grade metamorphic rocks and as authi-

genic albite in certain sedimentary varieties.<sup>23</sup> In our samples the authigenic form is likely to occur in muscovite–albite granite form. Muscovite can be usually found in sedimentary rocks rather than in igneous rocks of intermediate, mafic, and ultramafic composition,<sup>24</sup> but this kind of rocks with higher metals content could be also found in near region as Posavina.<sup>25</sup>

Decreasing of quartz mechanisms binding of heavy metals (dominantly Cu and Cd) is replaced by phyllosilicate, illite and albite (Fig. 7), which during the hydrothermal alteration in combination with oxidation, pH values and different precipitations and weathering conditions could act like zeolites based minerals with high capacity of long term capturing of pillar heavy metals clusters. Not dominant, but present, CHS polzonitic reactions occur in heterogeneous sediment structure in investigated Begej Canal locations, with cross border pollution.<sup>26</sup> The CaCO<sub>3</sub> content in this region is high and varies from 9.2 to 31.8 % (average 19.3 %)<sup>16</sup> and consequently it can be assumed, that the genesis of CSH and related polzonitic reactions could be time related including dependence from higher temperature, pressure, pH and other geochemical parameters. This could be the reason for encapsulating of heavy metals, including Cu and Cd in the river bed and later in landfill sediment site.

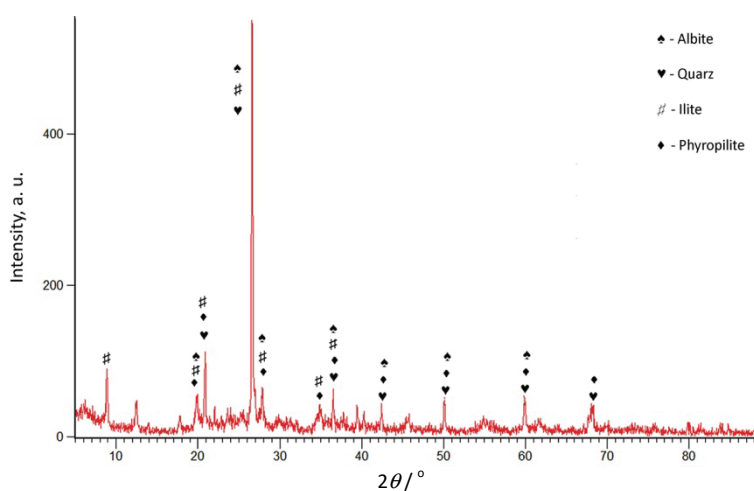


Fig. 7. The dominant selected minerals from sample 2 (2018).

These mineral complexations will lead to higher maturation as demonstrated in Table III and Fig. 8 in 2019 with potential encapsulation of Cu and Cd in mineral phases. Fig. 8 shows quartz and illite as dominant peaks and from Table III silicon oxide, carbonates and aluminosilicates. The Cd and Cu captured in minerals are not available in free forms in sediment or water.

Literature data show that muscovite and illite have high heavy metals adsorption capacity.<sup>27</sup> The results show that for, *e.g.*, Cu<sup>2+</sup> and Zn<sup>2+</sup> are adsorbed as



monovalent ions, probably as  $(\text{CuOH})^{+1}$  and  $(\text{ZnOH})^{+1}$  hydroxy surface complexes, due to their high ionic potential. SEM/EDS pushes a higher content of Al, Si, which confirms aluminosilicate sheets, as well as Ca and heavy metals, *e.g.*, Cu and Cd higher content in Figs. 3–5.

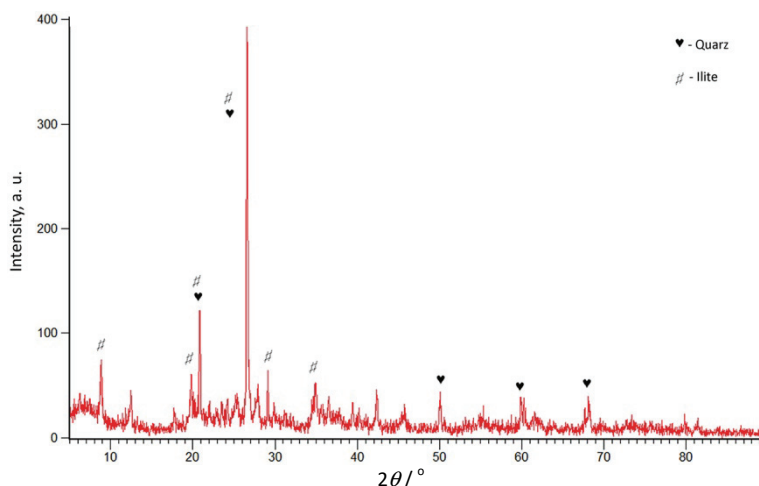


Fig. 8. The dominant selected minerals from sample 3 (2019).

TABLE III. Dominant related and other compounds in sample 3 (2019)

Compound name	Chemical formula
<b>Silicon oxide</b>	<b><math>\text{SiO}_2</math></b>
<b>Calcium carbonate</b>	<b><math>\text{Ca}(\text{CO}_3)</math></b>
Copper sulfate hydroxide hydrate	$\text{Cu}_4(\text{SO}_4(\text{OH})_6\text{H}_2\text{O})\text{H}_2\text{O}$
<b>Sodium aluminum silicate</b>	<b><math>\text{NaAlSiO}_4</math></b>
Aluminum tetrahydroxodisilicate formamide	$\text{Al}_2\text{Si}_2\text{O}_5(\text{OH})_4(\text{HCONH}_2)$
Gallium cadmium copper oxide	$\text{Ga}_2\text{Cd}_{.75}\text{Cu}_{.25}\text{O}_4$
Copper hydroxide sulfate hydrate	$\text{Cu}_{15}(\text{OH})_{22}(\text{SO}_4)_4(\text{H}_2\text{O})_6$
Copper zinc sulfate hydroxide hydrate	$(\text{Cu}_6\text{Zn})(\text{SO}_4)_2(\text{OH})_{10}(\text{H}_2\text{O})_3$
Copper silicate hydroxide	$\text{Cu}_5\text{Si}_4\text{O}_{12}(\text{OH})_2$
Potassium aluminum silicate hydroxide	$\text{KA}_{12}(\text{Si}_3\text{Al})\text{O}_{10}(\text{OH})_2$

#### CONCLUSION

The long-term characterization of sediment from the landfill after dredging activity is presented, in order to determine the potential bioavailability of Cu and Cd metals characterized as a potential risk in the examined matrix. Using sequential BCR extraction, it was observed that the maturation of the deposited sludge leads to a decrease in the metal content in the available sediment fraction. This distribution of metals indicates that during the maturation of the landfill, metals are incorporated into stable mineral forms and thus become less available in other environmental media due to potential atmospheric influences. The application of

SEM/EDS and XRF analysis has contributed to the quantification of elements of interest such as Al and Si. Increase in the percentage of Si, suggests that the maturation of the landfill in the sediment is dominated by silicate compounds, and consequently the metals changed into more stable forms what was confirmed by sequential analysis. Mineral changes were characterized by the formation of new minerals, detected by the formation of larger aggregates and recorded by a scanning electron microscope. Previous studies showed that non-clay minerals (quartz and albite) can act as a sinter raw material at low to higher range of temperature and pressure, and that clay minerals (muscovite and illite) are also good adsorbent of dominantly monovalent ions. Temperature, pH or pressure are the well-known parameters in the mechanism for the encapsulation of heavy metals, confirmed in this research. Also the most important process is mixing of sediment after dredging that showed the high level results only few months after applying the best available technique (BAT). This could be taken into account for further analysis on implementing plan for longtime waste disposal process.

## ИЗВОД

КАРАКТЕРИЗАЦИЈА ИЗМУЉЕНОГ СЕДИМЕНТА ТОКОМ РАЗЛИЧИТИХ ФАЗА  
САЗРЕВАЊА ДЕПОНИЈЕ

МИЛОШ ДУБОВИНА, НЕНАД ГРБА, ДЕЈАН КРЧМАР, ЈАСМИНА АГБАБА, СРЂАН РОНЧЕВИЋ, ЂУРЂА КЕРКЕЗ  
и БОЖО ДАЛМАЦИЈА

*Универзитет у Новом Саду, Природно–математички факултет, Департаман за хемију, биохемију и  
заштити животне средине, Трт Досијеја Обрадовића 3, 21000 Нови Саг*

У овом раду размотрен је дугорочни мониторинг депонованог седимента у животну средину како би се испитао механизам инкорпорирања Cu и Cd у минералним фракцијама и размотрила њихова биодоступност током сазревања депоније. Применом технике секвенцијалне екстракције, утврђена је доминантна заступљеност Cu и Cd у оксидованој и резидуалној фракцији што указује на низак ризик биодоступности поменутих метала у животној средини. Сазревање депонованог седимента указује да се садржај Cu и Cd смањује током времена у измењивој фракцији, а повећава у оксидованој. Рендгенске технике XRF и EDS су показале доминантну заступљеност силиката у испитиваним узорцима, као и на могућност формирања силикатних једињења која имају способност да везују метале и тиме их преводе у мање мобилне форме у седименту. Снимајући узорке скенирајућим електронским микроскопом утврђено је формирање хетерогених структура током времена, што потврђује формирање нових минерала и потенцијалну могућност инкорпорирања бакра и кадмијума у њима. Како би се утврдиле минералне форме и доминантна једињења у испитиваним узорцима седимента, примењена је рендгенска дифракциона анализа и појашњени су путеви трансформације датих једињења током времена.

(Примљено 30. августа, ревидирано и прихваћено 29. новембра 2021)

## REFERENCES

1. R. L. Rudnick, S. Gao, in *Treatise on Geochemistry, Vol. 3: The Crust*, R. L. Rudnick, Ed., Elsevier Science, 2004, pp. 1–64 (<https://doi.org/10.1016/B0-08-043751-6/03016-4>)

2. S. R. Taylor, S. M. McLennan, *Rev. Geophys.* **33** (1995) 241 (<https://doi.org/10.1029/95RG00262>)
3. I. Ahumada, A. Maricán, M. Retamal, C. Pedraza, L. Ascar, A. Carrasco, P. Richter, *J. Braz. Chem. Soc.* **21** (2010) 721 (<https://doi.org/10.1590/S0103-50532010000400020>)
4. G. Rauret, J.F. Lopez-Sanchez, A. Sahuquillo, R. Rubio, C. Davidson, A. Ure, P. Quevauviller, *J. Environ. Monit.* **1** (1999) 57 (<https://doi.org/10.1039/A807854H>)
5. D. Rađenović, *PhD Thesis*, University of Novi Sad, Novi Sad, 2020 (<https://www.cris.uns.ac.rs/record.jsf?recordId=114883&source=NaRDuS&language=sr>) (in Serbian)
6. N. Varga, *PhD Thesis*, University of Novi Sad, Novi Sad, 2017 ([https://nardus.mpn.gov.rs/bitstream/handle/123456789/8627/Disertacija\\_11467.pdf?sequence=6&isAllowed=y](https://nardus.mpn.gov.rs/bitstream/handle/123456789/8627/Disertacija_11467.pdf?sequence=6&isAllowed=y)) (in Serbian)
7. R. Zhang, F. Zeng, W. Liu, R.J. Zeng, H. Jiang, *J. Environ. Manage.* **53** (2014) 1119 (<https://doi.org/10.1007/s00267-014-0268-0>)
8. A. Sahuquillo, J. F. López-Sánchez, R. Rubio, G. Rauret, R. P. Thomas, C. M. Davidson, A. M. Ure, *Anal. Chim. Acta* **382** (1999) 317 ([https://doi.org/10.1016/S0003-2670\(98\)00754-5](https://doi.org/10.1016/S0003-2670(98)00754-5))
9. K. Nemati, N. K. A. Bakar, M. R. Abas, E. Sobhanzadeh, *J. Hazard. Mater.* **192** (2011) 402 (<https://doi.org/10.1016/j.jhazmat.2011.05.039>)
10. D. Rađenović, Đ. Kerkez, D. Tomašević-Pilipović, M. Dubovina, N. Grba, D. Krčmar, B. Dalmacija, *Sci. Total Environ.* **684** (2019) 186 (<https://doi.org/10.1016/j.scitotenv.2019.05.351>)
11. A. Q. R. Baron, in *Synchrotron Light Sources and Free-Electron Lasers*, E. Jaeschke, S. Khan, J. Schneider, J. Hastings, Eds., Springer, Cham, 2016, pp. 1643–1713 ([http://dx.doi.org/10.1007/978-3-319-14394-1\\_41](http://dx.doi.org/10.1007/978-3-319-14394-1_41))
12. Y. Juhua, C. Qiuwen, Z. Jianyun, Z. Jicheng, F. Chengxin, H. Liuming, S. Wenqing, Y. Wenyong, Z. Yinlong, *Sci. Total Environ.* **658** (2019) 501 (<https://doi.org/10.1016/j.scitotenv.2018.12.226>)
13. S. Pradhanang, *JIST* **19** (2014) 123 (<https://doi.org/10.3126/jist.v19i2.13865>)
14. B. A. Al-Mur, *Oceanologia* **62** (2020) 31 (<https://doi.org/10.1016/j.oceano.2019.07.001>)
15. A. V. Filqueiras, I. Lavilla, C. Bendicho, *J. Environ. Monit.* **4** (2002) 823 (<https://doi.org/10.1039/B207574C>)
16. D. Rađenović, Đ. Kerkez, D. Tomašević-Pilipović, M. Dubovina, N. Grba, D. Krčmar, B. Dalmacija, *Sci. Total Environ.* **684** (2019) 186 (<https://doi.org/10.1016/j.scitotenv.2019.05.351>)
17. A. M. Ziyath, P. Mahbub, A. Goonetilleke, M. O. Adebajo, S. Kokot, A. Oloyede, *J. Water Resour. Prot.* **3** (2011) 758 (<https://doi.org/10.4236/jwarp.2011.310086>)
18. Z. D. Mojović, *PhD Thesis*, University of Belgrade, Belgrade, 2009 ([fedorabg.bg.ac.rs/fedora/get/o:7915/bdef:Content/get](http://fedorabg.bg.ac.rs/fedora/get/o:7915/bdef:Content/get)) (in Serbian)
19. R. Sánchez-Hernández, I. Padilla, S. López-Andrés, A. LópezDelgado, *Desalination Water Treat.* **126** (2018) 181 (<https://doi.org/10.5004/dwt.2018.22816>)
20. I. Obreht, C. Zeeden, P. Schulte, U. Hambach, E. Eckmeier, A. Timar-Gabor, F. Lehmkuhl, *Aeolian Res.* **18** (2015) 69 (<https://doi.org/10.1016/j.aeolia.2015.06.004>)
21. B. Lothenbach, E. Bernard, U. Mäder, *Phys. Chem. Earth* **99** (2017) 77 (<https://doi.org/10.1016/j.pce.2017.02.006>)

22. S. Salimkhani, K. Siahcheshm, A. Kadkhodaie, H. Salimkhani, *Mater. Chem. Phys.* **271** (2021) 124 (<https://doi.org/10.1016/j.matchemphys.2021.124957>)
23. *Albite*, <https://www.britannica.com/science/albite> (accessed August 10, 2021)
24. *Muscovite*, <https://geology.com/minerals/muscovite.shtml> (accessed August 10, 2021)
25. N. Grba, F. Neubauer, A. Šajnović, K. Stojanović, B. Jovančičević, *J. Serb. Chem. Soc.* **80** (2015) 827 (<https://doi.org/10.2298/JSC140317047G>)
26. M. Dubovina, D. Krčmar, N. Grba, M. A. Watson, D. Rađenović, D. Tomašević-Pilipović, B. Dalmacija, *Environ. Pollut.* **236** (2018) 773 (<https://doi.org/10.1016/j.envpol.2018.02.014>)
27. S. Gier, W. D. Johns, *Appl. Clay Sci.* **16** (2000) 289 ([https://doi.org/10.1016/S0169-1317\(00\)00004-1](https://doi.org/10.1016/S0169-1317(00)00004-1)).